Two-photon blockade generated and enhanced by mechanical squeezing

Ling-Juan Feng [1,*] and Shang-Qing Gong [2,†]

[1]*College of Sciences, Shanghai Institute of Technology, 100 Haiquan Road, Shanghai 201418, China*
[2]*Department of Physics, East China University of Science and Technology, Shanghai 200237, China*

Photon blockade is an important quantum nonlinear phenomenon in cavity optomechanics. Here, we investigate the two-photon blockade effect by exploiting the mechanical squeezing. This squeezing can enhance the optomechanical-coupling strength into the single-photon strong-coupling regime. With strong coupling, we find the photon blockade effects can be generated and enhanced, and the region where the two-photon blockade occurs can be widened. Finally, we study the transition between photon-induced tunneling and blockade.

I. INTRODUCTION

Cavity optomechanics [1–6], exploring the radiation-pressure-induced interaction between light and mechanical motion on the macroscopic scale, has progressed enormously in the past few years. Examples include optomechanical cooling [7,8], optomechanically induced transparency [9–12], coherent photon-phonon conversion [13,14], squeezed light [15–17], nonreciprocal optical transmission [18–20], or, most relevant to this study, photon blockade [21–34], which was first proposed by Rabl *et al.* [21,22].

Generally, the conventional photon blockade relies mainly on the anharmonicity of the energy structure [35,36]. This originates from the nonlinear optomechanical coupling in optomechanical systems. Based on the nonlinearity, especially the Kerr-type nonlinearity, earlier works have examined the photon blockade effect in the single-photon strong-coupling regime [21–34]. In such a regime, the single-photon optomechanical-coupling strength is much larger than the system losses. However, in the current experiments, it is difficult to realize this strong coupling on the single-photon level. To overcome the obstacle, people have proposed some theoretical schemes to enhance the coupling strength, such as optical coalescence [37], Josephson effect [38–40], and squeezing effect of the cavity or mechanical mode [31,32].

Recently, two-photon blockade, i.e., the absorption of two photons that blocks the absorption of subsequent photons, has attracted a great deal of attention in the various configurations [23,33,34,41–43]. For example, this blockade can be generated and enhanced in the optomechanical system with the optical parametric amplification or the external mechanical pumping [33,34]. Different from the above studies [33,34], we investigate the two-photon blockade effect with the mechanical squeezing in the nonlinear hybrid optomechanical system [44–48]. This squeezing is realized through the Coulomb interaction between the charged mechanical oscillator and the

charged body, which is experimentally feasible [49–56]. It could produce the strong optomechanical-coupling strength sufficient for the realization of energy-level anharmonicity. Through calculating the higher-order correlation functions, we find that the strong optomechanical coupling can generate and enhance the blockade effects and can widen the region of two-photon blockade. Moreover, by varying the optomechanical coupling, photon-induced tunneling can be converted into photon blockade, or vice versa. Therefore, our proposed scheme offers an alternative approach to achieve the high-quality and efficient few-photon sources.

II. THEORETICAL MODEL

A cavity optomechanical system [44–48] depicted in Fig. 1 consists of an optomechanical cavity and a charged body outside. The charged mechanical oscillator couples to the cavity field via the radiation pressure force and interacts with the charged body via the Coulomb force. The cavity from the fixed mirror is driven by a weak probe field with frequency ω_l and amplitude ε_l. In a frame rotating with ω_l, the Hamiltonian describing this system is given by

$$H = H_0 + H_{\mathrm{om}} + H_{\mathrm{co}} + H_{\mathrm{pr}}, \qquad (1)$$

where

$$H_0 = \hbar\Delta a^\dagger a + \frac{1}{2}m\omega_m^2 x^2 + \frac{p^2}{2m},$$

$$H_{\mathrm{om}} = -\hbar g_0 a^\dagger a x,$$

$$H_{\mathrm{co}} = -\frac{k_e C_1 \mathrm{U}_1 C_2 \mathrm{U}_2}{|r_0 + x|},$$

$$H_{\mathrm{pr}} = \hbar\varepsilon_l(a^\dagger + a).$$

Here a ($a^\dagger$) and x (p) are the annihilation (creation) operator of the cavity mode, and the position (momentum) operator of the mechanical oscillator mode with frequency ω_m and mass m,

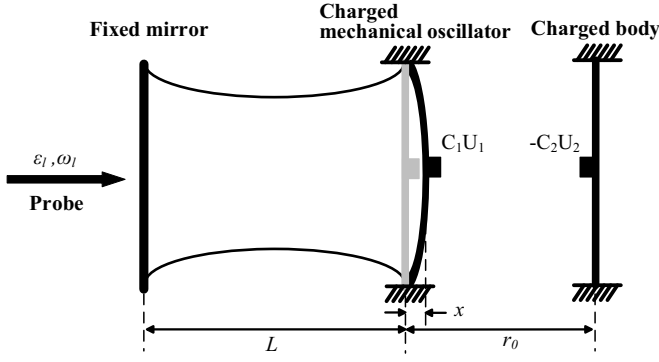*lingjuanfeng@sit.edu.cn
†sqgong@ecust.edu.cn

FIG. 1. Schematic representation of a cavity optomechanical system, where an optomechanical cavity is coupled to a charged body through the Coulomb force.

respectively. $\Delta = \omega_c - \omega_l$ is the detuning between the cavity mode (frequency ω_c) and the probe field. $g_0 = \omega_c/L$ denotes the optomechanical coupling strength with L being the cavity length. k_e is the electrostatic constant. $C_1 U_1$ is the positive charge on the charged mechanical oscillator, and $-C_2 U_2$ is the negative charge on the charged body, with C_1 (C_2) and U_1 ($-U_2$) being the capacitance and the bias gate voltage, respectively. r_0 represents the equilibrium separation between the charged mechanical oscillator and the charged body, in the absence of the radiation pressure and the Coulomb force.

In the case of $x \ll r_0$, H_{co} can be expanded to second order of x/r_0 as $-\frac{k_e C_1 U_1 C_2 U_2}{r_0}[1 - \frac{x}{r_0} + \frac{x^2}{r_0^2}]$ [50,51]. The linear term proportional to x may be absorbed into the definition of the equilibrium position. By further omitting the constant term, we then obtain a simple form $H_{co} = -\frac{k_e C_1 U_1 C_2 U_2}{r_0^3}x^2$.

Introducing position and momentum operators for the vibration mode of mechanical oscillator as $x = [\hbar/(2m\omega_m)]^{1/2}(b^\dagger + b)$ and $p = i[\hbar m\omega_m/2]^{1/2}(b^\dagger - b)$, H can be written as

$$H' = \hbar\Delta a^\dagger a + \hbar(\omega_m - 2G)b^\dagger b - \hbar g a^\dagger a(b^\dagger + b)$$
$$- \hbar G(b^{\dagger 2} + b^2) + \hbar\varepsilon_l(a^\dagger + a), \quad (2)$$

where $g = \frac{\omega_c}{L}\sqrt{\hbar/2m\omega_m}$ is the coupling strength, $G = k_e C_1 U_1 C_2 U_2/(2m\omega_m r_0^3)$ is the effective mechanical coupling constant, and b ($b^\dagger$) is the annihilation (creation) operator of the mechanical oscillator mode. In Eq. (2), we have neglected the zero-point energy from the second term.

To obtain strong optomechanical coupling, we need to use the squeezing of mechanical oscillator mode [32]. In terms of a squeezing transformation $b = \cosh(r)b_s + \sinh(r)b_s^\dagger$, with a preferred squeezed mechanical mode b_s and a squeezing parameter $r = (1/4)\ln[\omega_m/(\omega_m - 4G)]$, H' is transformed to a standard optomechanical Hamiltonian

$$H_{OMS} = \hbar\Delta a^\dagger a + \hbar\omega_s b_s^\dagger b_s - \hbar g_s a^\dagger a(b_s^\dagger + b_s)$$
$$+ \hbar\varepsilon_l(a^\dagger + a). \quad (3)$$

Here, the second and fourth terms in Eq. (2) have been diagonalized by the squeezing transformation and are simplified to a mechanical oscillator ($\hbar\omega_s b_s^\dagger b_s$) in Eq. (3) with a transformed mechanical frequency $\omega_s = (\omega_m - 4G)\exp(2r)$. $g_s = g\exp(r)$ describes the single-photon optomechanical-coupling
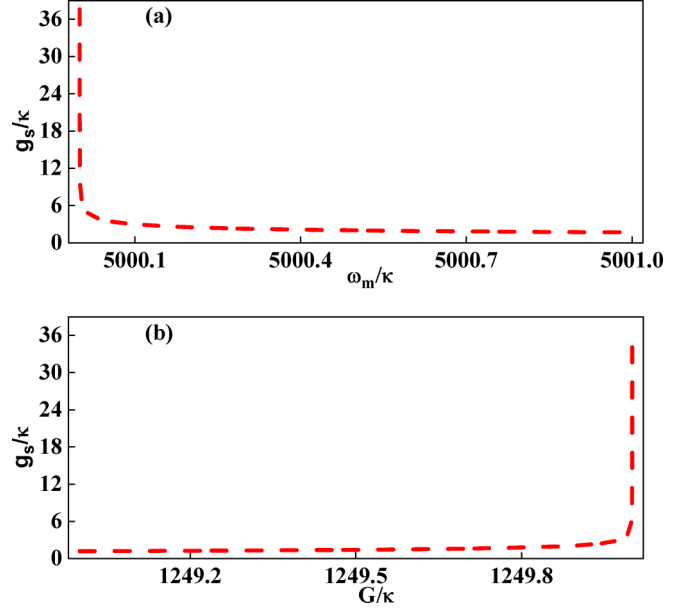

FIG. 2. The optomechanical coupling strength g_s/κ versus the mechanical frequency ω_m and the coupling G. The parameters are scaled by the cavity decay rate κ, i.e., $g = 0.2\kappa$, (a) $G = 1250\kappa$, and (b) $\omega_m = 5000\kappa$.

strength, which could be significantly enhanced by adjusting properly the mechanical frequency ω_m and the effective mechanical coupling constant G, as shown in Fig. 2. In other words, the optomechanical coupling between the squeezed mechanical mode and the cavity mode can reach the single-photon strong-coupling regime $g_s > \kappa$, even when the system is originally in the weak-coupling regime $g < \kappa$.

In a rotating reference frame defined by the unitary transformation $U = \exp(-i\omega_s b_s^\dagger b_s t)$, H_{OMS} is reduced to

$$H'_{OMS} = \hbar\Delta a^\dagger a - \hbar g_s a^\dagger a(b_s^\dagger e^{i\omega_s t} + b_s e^{-i\omega_s t})$$
$$+ \hbar\varepsilon_l(a^\dagger + a). \quad (4)$$

In the limit $\omega_s \gg g_s$, we can adiabatically eliminate the mechanical mode $b_s^\dagger$ and b_s and obtain the effective Hamiltonian [57–59]

$$H_{eff} = \hbar\Delta a^\dagger a + \hbar\tilde{g}a^\dagger a a^\dagger a + \hbar\varepsilon_l(a^\dagger + a), \quad (5)$$

where $\tilde{g} = g_s^2/\omega_s$ is the photon-photon coupling strength. Furthermore, the above Hamiltonian can be rewritten as follows:

$$H_{eff}^k = \hbar\Delta_k a^\dagger a + \hbar\tilde{g}a^\dagger a(a^\dagger a - k) + \hbar\varepsilon_l(a^\dagger + a), \quad (6)$$

where $\Delta_k = \omega_c - \omega_l + k\tilde{g}$ is the frequency mismatch, and k is the positive tuning parameter, as in Ref. [23]. In the weak-probe regime, we have the eigensystem $H_{eff}^k|n\rangle = E_n|n\rangle$, with eigenvalues

$$E_n = n\hbar\Delta_k + n^2\hbar\tilde{g} - nk\hbar\tilde{g}, \quad (7)$$

and the harmonic-oscillator number state of the cavity mode $|n\rangle$. From Eq. (7), we notice that the energy difference $\Delta E = E_{n+1} - E_n$ is not constant, which indicates the anharmonicity of the energy structure. This is the origin of conventional n-photon blockade and is illustrated in more detail in Fig. 3. If
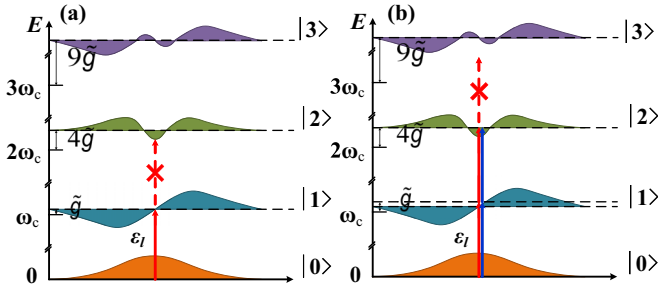
FIG. 3. Schematic energy-level diagram of the isolated, single-mode optomechanical system: (a) single-photon blockade, and (b) two-photon blockade or photon-induced tunneling.

the probe beam is on resonance with the $|0\rangle \rightarrow |1\rangle$ transition, i.e., $\omega_l = \omega_c + \tilde{g}$ ($k = 1$), the $|1\rangle \rightarrow |2\rangle$ transition is detuned by $2\hbar\tilde{g}$ and will be suppressed for the strong-coupling regime of $\tilde{g} > \kappa$, which features single-photon blockade, as shown in Fig. 3(a). Similarly, two-photon blockade can occur when the two-photon-resonance condition ($k = 2$) is satisfied, as denoted by red arrows in Fig. 3(b). The $|0\rangle \rightarrow |2\rangle$ transition is resonantly driven by the probe beam, but the $|2\rangle \rightarrow |3\rangle$ transition is detuned by $3\hbar\tilde{g}$. Moreover, two-photon blockade corresponds to photon-induced tunneling, as denoted by blue arrows in Fig. 3(b). This indicates that the absorption of the first photon favors also that of the second photon.

III. PHOTON BLOCKADE AND PHOTON-INDUCED TUNNELING

Next, we study photon blockade and photon-induced tunneling by using the equal-time (namely, zero time delay) nth-order correlation function

$$g^{(n)}(0) = \frac{\langle a^{\dagger n} a^n \rangle}{\langle a^\dagger a \rangle^n} \text{ for } n \geqslant 2. \tag{8}$$

Accordingly, the second-order and third-order correlation functions are $g^{(2)}(0) = \langle a^{\dagger 2} a^2 \rangle / \langle a^\dagger a \rangle^2$ and $g^{(3)}(0) = \langle a^{\dagger 3} a^3 \rangle / \langle a^\dagger a \rangle^3$, respectively. To describe photon blockade and photon-induced tunneling quantitatively, we use the following criteria:

1. $g^{(2)}(0) < 1$ represents the sub-Poisson statistics of the cavity field, which is the photon antibunching effect. The limit $g^{(2)}(0) \rightarrow 0$ means the complete photon blockade (1PB), where two photons (or multiple photons) never occupy the cavity at the same time.

2. $g^{(2)}(0) > 1 > g^{(3)}(0)$ corresponds to two-photon blockade (2PB), which implies two-photon bunching and three-photon antibunching.

3. $g^{(n)}(0) > 1$ indicates the super-Poisson statistics of the cavity field, which is the photon bunching effect. This characterizes the photon-induced tunneling (PIT).

A. Analytical results

We phenomenologically add the dissipation term of the cavity mode to H_{eff}^k, and then obtain the effective non-Hermitian Hamiltonian

$$H_{\text{eff}}' = H_{\text{eff}}^k - i\hbar\frac{\kappa}{2} a^\dagger a, \tag{9}$$

where this Hamiltonian can be expressed in a spectral representation as

$$\begin{aligned}
H_{\text{eff}}' &= \sum_{n=0}^{\infty} \left(E_n - i\hbar\frac{\kappa}{2} n \right) |n\rangle\langle n| \\
&\quad + \hbar\varepsilon_l \sum_{n=0}^{\infty} |n\rangle\langle n|(a^\dagger + a) \sum_{n'=0}^{\infty} |n'\rangle\langle n'| \\
&= \sum_{n=0}^{\infty} \left(E_n - i\hbar\frac{\kappa}{2} n \right) |n\rangle\langle n| \\
&\quad + \hbar\varepsilon_l \sum_{n=0}^{\infty} \sqrt{n+1}(|n+1\rangle\langle n| + |n\rangle\langle n+1|). \tag{10}
\end{aligned}$$

For the weak-probe case, $\varepsilon_l/\kappa \ll 1$, only the lower energy levels of the cavity field are excited. Thus, in the few-photon subspace, the general state can be written as

$$|\varphi(t)\rangle = C_0(t)|0\rangle + C_1(t)|1\rangle + C_2(t)|2\rangle, \tag{11}$$

where the coefficient $C_n(t)$ is the probability amplitude, with photon numbers $n = 0, 1, 2$. Correspondingly, the Hamiltonian in Eq. (10) becomes

$$\begin{aligned}
H_{\text{eff}}' &= E_0|0\rangle\langle 0| + \left(E_1 - i\hbar\frac{\kappa}{2} \right)|1\rangle\langle 1| + (E_2 - i\hbar\kappa)|2\rangle\langle 2| \\
&\quad + \hbar\varepsilon_l(|1\rangle\langle 0| + |0\rangle\langle 1|) + \sqrt{2}\hbar\varepsilon_l(|2\rangle\langle 1| + |1\rangle\langle 2|), \tag{12}
\end{aligned}$$

where $E_0 = 0$, $E_1 = \hbar\Delta + \hbar\tilde{g}$, and $E_2 = 2\hbar\Delta + 4\hbar\tilde{g}$.

In terms of Eqs. (11) and (12), and the Schrödinger equation $i\hbar d|\varphi(t)\rangle/dt = H_{\text{eff}}'|\varphi(t)\rangle$, we can obtain the following equations of motion for the probability amplitudes:

$$\begin{aligned}
i\hbar\dot{C}_0(t) &= E_0 C_0(t) + \hbar\varepsilon_l C_1(t), \\
i\hbar\dot{C}_1(t) &= \hbar\varepsilon_l C_0(t) + \left(E_1 - i\hbar\frac{\kappa}{2} \right)C_1(t) + \sqrt{2}\hbar\varepsilon_l C_2(t), \\
i\hbar\dot{C}_2(t) &= \sqrt{2}\hbar\varepsilon_l C_1(t) + (E_2 - i\hbar\kappa)C_2(t). \tag{13}
\end{aligned}$$

Due to the weak-probe limit, we have the approximate expressions: $C_0 \approx 1$, $C_1 \sim \varepsilon_l/\kappa$, $C_2 \sim \varepsilon_l^2/\kappa^2$, and then can approximately solve the equations in Eq. (13) by discarding the higher-order terms of ε_l. Assume that the cavity is initially in the vacuum state, i.e., $C_0(0) = 1$, the long-time (steady state) solutions of the equations of motion for the probability amplitudes can be obtained:

$$\begin{aligned}
C_0(\infty) &\equiv C_0 = 1, \\
C_1(\infty) &\equiv C_1 = \frac{-\varepsilon_l}{(E_1/\hbar - i\kappa/2)}, \\
C_2(\infty) &\equiv C_2 = \frac{\sqrt{2}\varepsilon_l^2}{(E_2/\hbar - i\kappa)(E_1/\hbar - i\kappa/2)}. \tag{14}
\end{aligned}$$

For the state given in Eq. (11), the second-order correlation function can be written as

$$\begin{aligned}
g^{(2)}(0) &= \frac{\sum_{n,n'=0}^{2} C_n^* C_{n'} \langle n|(a^{\dagger 2} a^2)|n'\rangle}{\left(\sum_{n,n'=0}^{2} C_n^* C_{n'} \langle n|a^\dagger a|n'\rangle \right)^2} \\
&= \frac{2P_2}{N(P_1 + 2P_2)^2}, \tag{15}
\end{aligned}$$

where $N = 1 + |C_1|^2 + |C_2|^2$ is the normalization coefficient of the state, $P_1 = |C_1|^2/N$ and $P_2 = |C_2|^2/N$ are the probabilities for finding a single photon and two photons in the cavity, respectively. Since the probe field is sufficiently weak, we have $N \approx 1$ with $|C_2|^2 \ll |C_1|^2 \ll 1$. Hence, the second-order correlation function is approximately given by

$$g^2(0) \approx \frac{2P_2}{P_1^2} = \frac{\kappa^2/4 + (\tilde{g} + \Delta)^2}{\kappa^2/4 + (2\tilde{g} + \Delta)^2}. \quad (16)$$

For the single-photon resonant excitation from the ground state to the first-excited state of the cavity field, i.e., $\Delta = -\tilde{g}$ ($k = 1$), the second-order correlation function becomes $g^2(0) = [1 + 4\tilde{g}^2/\kappa^2]^{-1} < 1$. In the strong-coupling regime $\tilde{g}/\kappa > 1$, we have $g^2(0) \ll 1$, which indicates that 1PB can be achieved. For the two-photon resonant excitation from the ground state to the second-excited state of the cavity field, i.e., $\Delta = -2\tilde{g}$ ($k = 2$), the second-order correlation function becomes $g^2(0) = 1 + 4\tilde{g}^2/\kappa^2 > 1$, which corresponds to the PIT.

Similarly, we calculate the third-order correlation function in the steady-state case as

$$g^3(0) = \frac{[\kappa^2/4 + (\tilde{g} + \Delta)^2]^2}{[\kappa^2/4 + (2\tilde{g} + \Delta)^2][\kappa^2/4 + (3\tilde{g} + \Delta)^2]}. \quad (17)$$

B. Numerical results and discussion

We numerically study the systemic dynamics after taking into account optical and mechanical dissipations. The system master equation of the density operator ρ is given by

$$\dot{\rho} = \frac{i}{\hbar}[\rho, H] + \kappa \mathcal{D}[a]\rho + \gamma(N_s + 1)\mathcal{D}[b_s]\rho$$
$$+ \gamma N_s \mathcal{D}[b_s^\dagger]\rho + \gamma M_s \mathcal{G}[b_s]\rho + \gamma M_s^* \mathcal{G}[b_s^\dagger]\rho, \quad (18)$$

where κ and γ denote the cavity and mechanical decay rates, and the cavity field is in a vacuum bath. Here, $\mathcal{D}[o]\rho = o\rho o^\dagger - (o^\dagger o\rho + \rho o^\dagger o)/2$ and $\mathcal{G}[o]\rho = o\rho o - (oo\rho + \rho oo)/2$ are the standard dissipators in the Lindblad form. In addition, the expressions $N_s = \sinh^2(2r)[1 + \cos(\Phi)]/2$ and $M_s = -\sinh(2r)[1 + \exp(i\Phi)][\cosh^2(r) + \exp(-i\Phi)\sinh^2(r)]/2$ correspond to the effective thermal noise and the strength of the two-phonon correlation for the squeezed mechanical mode b_s [60]. Note that, when the ideal parameter condition $\Phi = \pm n\pi$ ($n = 1, 3, 5, \ldots$), the thermal noise and the two-phonon correlation strength can be suppressed completely; that is, $N_s, M_s = 0$.

To check the validity of the effective Hamiltonian H_{eff}, in Fig. 4 we plot the evolution of the correlation function $g^{(2)}(0)$. It clearly shows that the numerical result corresponding to the effective Hamiltonian H_{eff} (green dots) agrees well with the exact numerical calculation obtained using the full Hamiltonian H_{OMS} (red curve). We also find that the correlation function $g^{(2)}(0)$ approaches a steady value at $\kappa t \approx 15$. For $\kappa = 0.1$ MHz, the relaxation time of the system is about $150 \, \mu$s.

Figure 5 displays the correlation functions $g^{(2)}(0)$ and $g^{(3)}(0)$ as functions of the detuning Δ/κ without and with
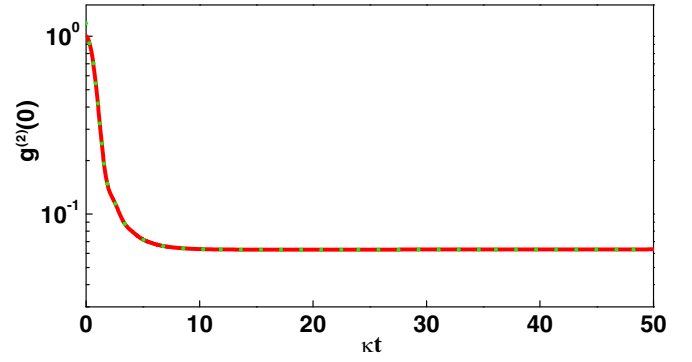

FIG. 4. The second-order correlation function $g^{(2)}(0)$ versus the scaled time κt in the case of single-photon resonance (i.e., $\Delta = -\tilde{g}$) and the ideal parameter condition (i.e., $\Phi = \pi$). Here, the results are obtained by numerically calculating master Eq. (18) with H_{eff} and H_{OMS}. Parameters are chosen as $\omega_s = 2000\kappa$, $g_s = 20\sqrt{10}\kappa$, $\gamma = 10^{-3}\kappa$, and $\varepsilon_l = 0.1\kappa$.

the mechanical squeezing, respectively. Here, the solid curves show the approximate analytical results based on Eqs. (16) and (17), while the red circles are based on the numerical results of the master equation in Eq. (18). We find that the analytical results are in an excellent agreement with the numerical results. Specifically, without the mechanical squeezing ($G = 0$), i.e., in the weak-coupling regime, there is no photon
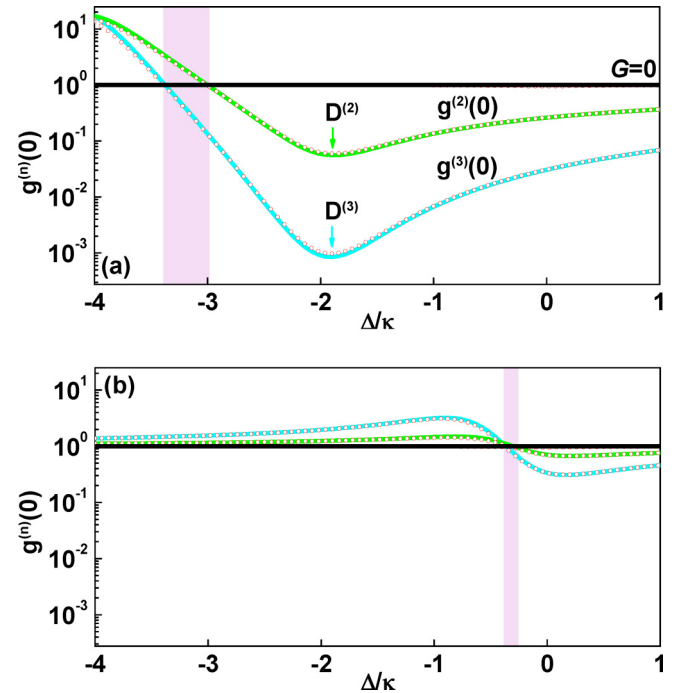

FIG. 5. The second- and third-order correlation functions $g^{(2)}(0)$ and $g^{(3)}(0)$ versus the detuning Δ/κ. (a) $\delta = 0.02\kappa$ and (b) $\delta = 0.2\kappa$. Here, the symbol δ denotes the difference between the parameters ω_m and $4G$ as $\delta = \omega_m - 4G$. $D^{(2)}$ and $D^{(3)}$ are the dips in the $g^{(2)}(0)$ and $g^{(3)}(0)$, respectively. The pink regions indicate the occurrence of two-photon blockade. Other parameters are taken as $\omega_m = 5000\kappa$, $g = 0.2\kappa$, and $\varepsilon_l = 0.1\kappa$.
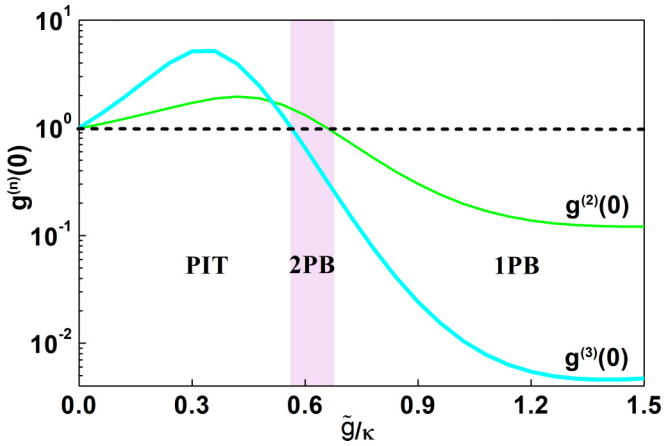
FIG. 6. The second- and third-order correlation functions $g^{(2)}(0)$ given in Eq. (16) and $g^{(3)}(0)$ given in Eq. (17) versus the coupling $\tilde{g}/\kappa$. The parameters are the same as in Fig. 5 except for the detuning $\Delta/\kappa = -1$.

blockade effect. That is because the weak coupling cannot cause the sufficient anharmonicity, resulting in the incomplete suppression of multiphoton excitation. However, in the presence of the mechanical squeezing, we find that single-photon blockade and two-photon blockade effects can emerge by varying the parameter δ. Obviously, as δ decreases, the photon blockade effects are significantly enhanced, and the regions where two-photon blockade occurs are widened. That is because the small δ could produce the strong optomechanical coupling sufficient for the realization of the anharmonicity. Thus, the strong optomechanical coupling is necessary for generating and enhancing photon blockade effects. Moreover, with the increase of the optomechanical coupling $\tilde{g}$, the photon-induced tunneling (PIT) effect can be transformed into the photon blockade (2PB and 1PB) effects for $\Delta/\kappa = -1$, which can be seen more clearly in Fig. 6. This transition induced by the optomechanical coupling (the mechanical squeezing) would be helpful for exploring quantum control of antibunching and bunching light.

IV. EXPERIMENTAL FEASIBILITY AND CONCLUSION

To generate and enhance photon blockade effects, the strong-coupling condition $g_0 > \kappa$ must be satisfied. However, until now this condition in the experiments is still a big challenge. Fortunately, in our proposal, the optomechanical coupling can be enhanced into the single-photon strong-coupling regime by the mechanical squeezing, even if the system is originally in the weak-coupling regime. Specifically, we choose the realistic parameters [44–56] as $C_1 = C_2 = 27.5$ nF, $U_1 = U_2 = 1$ V, $r_0 = 67$ μm, and then obtain the effective mechanical coupling constant $G \approx$ GHz. Moreover, micro- and nanofabricated optomechanical systems [61–65] have already demonstrated the high mechanical frequency $\omega_m \approx$ GHz. When ω_m infinitely approaches $4G$, we obtain a large squeezing parameter r. This leads to the realization of the strong optomechanical coupling. Thus, we believe that the proposal could be implemented on the currently available experimental technologies.

In summary, we have investigated the enhanced two-photon blockade effect via the mechanical squeezing, in the optomechanical system consisting of charged mechanical oscillator coupled with cavity field and charged body. Due to this squeezing, the optomechanical coupling can be significantly enhanced into the single-photon strong-coupling regime, which can cause the sufficient anharmonicity. By analytically and numerically calculating the correlation functions, we have found that the strong optomechanical coupling not only enhances the photon blockade effects but also widens the region where the two-photon blockade occurs. Furthermore, we have shown that the transition from photon-induced tunneling to photon blockade can be achieved by increasing the coupling. Finally, the basic mechanism of our work can be extended to the other blockade effects, such as phonon blockade or magnon blockade.

[1] T. J. Kippenberg and K. J. Vahala, Science **321**, 1172 (2008).

[2] F. Marquardt and S. M. Girvin, Physics **2**, 40 (2009).

[3] M. Aspelmeyer, P. Meystre, and K. Schwab, Phys. Today **65**(7), 29 (2012).

[4] P. Meystre, Ann. Phys. (Berlin, Ger.) **525**, 215 (2013).

[5] M. Aspelmeyer, T. J. Kippenberg, and F. Marquardt, Rev. Mod. Phys. **86**, 1391 (2014).

[6] W. P. Bowen and G. J. Milburn, *Quantum Optomechanics* (CRC Press, Boca Raton, 2016).

[7] S. Mancini, D. Vitali, and P. Tombesi, Phys. Rev. Lett. **80**, 688 (1998).

[8] P. Yanes-Thomas, P. Barberis-Blostein, and M. Bienert, Phys. Rev. A **102**, 013512 (2020).

[9] S. Weis, R. Rivière, S. Deléglise, E. Gavartin, O. Arcizet, A. Schliesser, and T. J. Kippenberg, Science **330**, 1520 (2010).

[10] G. S. Agarwal and S. Huang, Phys. Rev. A **81**, 041803(R) (2010).

[11] A. H. Safavi-Naeini, T. P. Mayer Alegre, J. Chan, M. Eichenfield, M. Winger, Q. Lin, J. T. Hill, D. E. Chang, and O. Painter, Nature (London) **472**, 69 (2011).

[12] X. B. Yan, Phys. Rev. A **101**, 043820 (2020).

[13] V. Fiore, Y. Yang, M. C. Kuzyk, R. Barbour, L. Tian, and H. Wang, Phys. Rev. Lett. **107**, 133601 (2011).

[14] E. Verhagen, S. S. Deléglise, S. Weis, A. Schliesser, and T. J. Kippenberg, Nature (London) **482**, 63 (2012).

[15] D. W. C. Brooks, T. Botter, S. Schreppler, T. P. Purdy, N. Brahms, and D. M. Stamper-Kurn, Nature (London) **488**, 476 (2012).

[16] A. H. Safavi-Naeini, S. Gröblacher, J. T. Hill, J. Chan, M. Aspelmeyer, and O. Painter, Nature (London) **500**, 185 (2013).

[17] T. P. Purdy, P. L. Yu, R. W. Peterson, N. S. Kampel, and C. A. Regal, Phys. Rev. X **3**, 031012 (2013).

[18] M. Hafezi and P. Rabl, Opt. Express **20**, 7672 (2012).

[19] Z. Shen, Y. L. Zhang, Y. Chen, C. L. Zou, Y. F. Xiao, X. B. Zou, F. W. Sun, G. C. Guo, and C. H. Dong, Nat. Photonics **10**, 657 (2016).

[20] X. B. Yan, H. L. Lu, F. Gao, and L. Yang, Front. Phys. **14**, 52601 (2019).

[21] P. Rabl, Phys. Rev. Lett. **107**, 063601 (2011).

[22] A. Nunnenkamp, K. Børkje, and S. M. Girvin, Phys. Rev. Lett. **107**, 063602 (2011).

[23] A. Miranowicz, M. Paprzycka, Y. X. Liu, J. Bajer, and F. Nori, Phys. Rev. A **87**, 023809 (2013).

[24] P. Kómár, S. D. Bennett, K. Stannigel, S. J. M. Habraken, P. Rabl, P. Zoller, and M. D. Lukin, Phys. Rev. A **87**, 013839 (2013).

[25] J. Q. Liao and F. Nori, Phys. Rev. A **88**, 023853 (2013).

[26] X. W. Xu and Y. J. Li, J. Phys. B: At., Mol. Opt. Phys. **46**, 035502 (2013).

[27] H. Wang, X. Gu, Y. X. Liu, A. Miranowicz, and F. Nori, Phys. Rev. A **92**, 033806 (2015).

[28] H. Xie, G. W. Lin, X. Chen, Z. H. Chen, and X. M. Lin, Phys. Rev. A **93**, 063860 (2016).

[29] F. Zou, L. B. Fan, J. F. Huang, and J. Q. Liao, Phys. Rev. A **99**, 043837 (2019).

[30] D. Y. Wang, C. H. Bai, S. Liu, S. Zhang, and H. F. Wang, Phys. Rev. A **99**, 043818 (2019).

[31] X. Y. Lü, Y. Wu, J. R. Johansson, H. Jing, J. Zhang, and F. Nori, Phys. Rev. Lett. **114**, 093602 (2015).

[32] T. S. Yin, X. Y. Lü, L. L. Zheng, M. Wang, S. Li, and Y. Wu, Phys. Rev. A **95**, 053861 (2017).

[33] C. Zhai, R. Huang, H. Jing, and L. M. Kuang, Opt. Express **27**, 27649 (2019).

[34] D. Y. Wang, C. H. Bai, X. Han, S. Liu, S. Zhang, and H. F. Wang, Opt. Lett. **45**, 2604 (2020).

[35] L. Tian and H. J. Carmichael, Phys. Rev. A **46**, R6801(R) (1992).

[36] A. Imamoglu, H. Schmidt, G. Woods, and M. Deutsch, Phys. Rev. Lett. **79**, 1467 (1997).

[37] C. Genes, A. Xuereb, G. Pupillo, and A. Dantan, Phys. Rev. A **88**, 033855 (2013).

[38] A. J. Rimberg, M. P. Blencowe, A. D. Armour, and P. D. Nation, New J. Phys. **16**, 055008 (2014).

[39] T. T. Heikkilä, F. Massel, J. Tuorila, R. Khan, and M. A. Sillanpää, Phys. Rev. Lett. **112**, 203603 (2014).

[40] J. R. Johansson, G. Johansson, and F. Nori, Phys. Rev. A **90**, 053833 (2014).

[41] C. Hamsen, K. N. Tolazzi, T. Wilk, and G. Rempe, Phys. Rev. Lett. **118**, 133604 (2017).

[42] Q. Bin, X. Y. Lü, S. W. Bin, and Y. Wu, Phys. Rev. A **98**, 043858 (2018).

[43] A. Kowalewska-Kudlaszyk, S. I. Abo, G. Chimczak, J. Perina, Jr., F. Nori, and A. Miranowicz, Phys. Rev. A **100**, 053857 (2019).

[44] J. Q. Zhang, Y. Li, M. Feng, and Y. Xu, Phys. Rev. A **86**, 053806 (2012).

[45] H. Xiong, Z. X. Liu, and Y. Wu, Opt. Lett. **42**, 3630 (2017).

[46] H. Xiong, L. G. Si, and Y. Wu, Appl. Phys. Lett. **110**, 171102 (2017).

[47] Z. X. Liu and H. Xiong, Sensors **18**, 3833 (2018).

[48] L. Li, W. X. Yang, Y. X. Zhang, T. Shui, A. X. Chen, and Z. M. Jiang, Phys. Rev. A **98**, 063840 (2018).

[49] D. Rugar and P. Grütter, Phys. Rev. Lett. **67**, 699 (1991).

[50] L. Tian and P. Zoller, Phys. Rev. Lett. **93**, 266403 (2004).

[51] W. K. Hensinger, D. W. Utami, H. S. Goan, K. Schwab, C. Monroe, and G. J. Milburn, Phys. Rev. A **72**, 041405(R) (2005).

[52] A. Szorkovszky, A. C. Doherty, G. I. Harris, and W. P. Bowen, Phys. Rev. Lett. **107**, 213603 (2011).

[53] A. Szorkovszky, G. A. Brawley, A. C. Doherty, and W. P. Bowen, Phys. Rev. Lett. **110**, 184301 (2013).

[54] J. Bochmann, A. Vainsencher, D. D. Awschalom, and A. N. Cleland, Nat. Phys. **9**, 712 (2013).

[55] L. Fan, K. Y. Fong, M. Poot, and H. X. Tang, Nat. Commun. **6**, 5850 (2015).

[56] C. Bekker, R. Kalra, C. Baker, and W. P. Bowen, Optica **4**, 1196 (2017).

[57] S. Mancini, V. I. Manko, and P. Tombesi, Phys. Rev. A **55**, 3042 (1997).

[58] S. Bose, K. Jacobs, and P. L. Knight, Phys. Rev. A **56**, 4175 (1997).

[59] D. F. V. James and J. Jerke, Can. J. Phys. **85**, 625 (2007).

[60] H. P. Breuer and F. Petruccione, *The Theory of Open Quantum Systems* (Clarendon Press, Oxford, 2002), Chap. 3.

[61] J. D. Thompson, B. M. Zwickl, A. M. Jayich, F. Marquardt, S. M. Girvin, and J. G. E. Harris, Nature (London) **452**, 72 (2008).

[62] A. Schliesser, R. Rivière, G. Anetsberger, O. Arcizet, and T. J. Kippenberg, Nat. Phys. **4**, 415 (2008).

[63] M. Eichenfield, J. Chan, R. M. Camacho, K. J. Vahala, and O. Painter, Nature (London) **462**, 78 (2009).

[64] J. C. Sankey, C. Yang, B. M. Zwickl, A. M. Jayich, and J. G. E. Harris, Nat. Phys. **6**, 707 (2010).

[65] J. Chan, T. M. Alegre, A. H. Safavi-Naeini, J. T. Hill, A. Krause, S. Gröblacher, M. Aspelmeyer, and O. Painter, Nature (London) **478**, 89 (2011).